JOURNAL OF AIRCRAFT
Vol. 35, No. 1, January–February 1998

Simple Numerical Method to Compute Viscous Lift Loss of Wings

R. S. Crabbe*
National Research Council, Ottawa K1A OR6, Canada

It is well known that the lift of a wing is less than the value computed on the basis of potential flow because of the presence of a boundary layer on the surface. A method of computing this lift loss is described based on numerically solving the integral equations of the three-dimensional boundary-layer flow in a streamline coordinate system. When applied to several swept, tapered, and twisted wings, the method closely predicts the lift curve measured in a wind tunnel. Similar computations with a two-dimensional (strip) model overestimate wing viscous lift loss by about 10%. The numerical effort required to solve the integral boundary-layer equation set is much less than that required to solve either the three-dimensional boundary-layer equations or the Navier–Stokes equations, with little loss in accuracy. It could easily be used, therefore, for preliminary estimates of climb and cruise wing performance. A simple procedure is presented for identifying crossflow separation.

Nomenclature

a	=	function in Eq. (11)
b	=	wing span
C_L	=	wing lift coefficient
c	=	local wing chord
c_f	=	skin-friction coefficient
$cpte$	=	pressure coefficient at the wing trailing edge
e	=	entrainment constant in Eq. (3)
H	=	boundary-layer shape factor
n	=	crossflow coordinate
s	=	streamline coordinate
u	=	streamwise boundary-layer velocity component
v	=	crossflow boundary-layer velocity component
X, Y, Z	=	global Cartesian coordinate system with X measured from the leading edge along the chord line in the plane of symmetry, and Y outboard perpendicular to this plane, Fig. 2
xte	=	value of x/c at the wing trailing edge
$x\emptyset$	=	defined by Eq. (11)
α	=	wing angle of attack
β	=	wall shear stress direction with respect to an external streamline
γ	=	streamline direction with respect to x
δ	=	boundary-layer thickness
δ^*	=	boundary-layer displacement thickness
ε	=	wall shear direction with respect to the x axis
λte	=	wing trailing-edge angle
σ	=	surface source strength
ω	=	relaxation constant

Introduction

THE presence of a boundary layer on a wing leads to a lift loss that is unlikely to be the same as sectional lift loss.[1,2] There are several reasons why this should be true, among them the fact that the pressure gradients are smaller on a wing than on a section, leading to lower boundary-layer thicknesses and hence, lift loss, and the fact that the boundary-layer displacement thickness may be less on a wing than on a section because of the three-dimensional nature of the wing boundary layer, which would again lead to lower lift loss. Because the boundary-layer flow, like the inviscid flow, on a wing is three dimensional, the resulting complexity of the equations has rendered their solution almost intractable. However, advances in applied mathematics in the last 20 years have yielded robust algorithms for the numerical integration of the nonlinear partial differential equation sets, and the advances in computing power exemplified by modern unix workstations have made implementation of the algorithms practicable. Navier–Stokes computational fluid dynamics (CFD) codes such as NPARC, CFD–ACE, CFDS–FLOW3D, and others, may therefore be employed to quantify the loss, but the computing architecture, necessity for a fine grid near the surface, pre-processing, etc., may limit their use to all but the most important cases. Commercial panel codes such as VSAERO are considered to be user friendly and reliable but are employed mainly for potential flow prediction inasmuch as their viscous code, at least as it applies to wings, is only approximate. In this paper, a relatively simple three-dimensional numerical model is presented that predicts viscous lift loss of wings, at least to engineering accuracy. For the cases discussed here, steady incompressible flow is assumed, although compressible pressure corrections can be implemented using the Karman–Tsien or Prandtl–Glauert rule.

The flow about a wing is three dimensional, as is the boundary layer, i.e., the boundary layer has crossflow. Cebeci et al.,[3] McLean,[4] and Matsuno[5] presented finite difference calculation procedures for computing three-dimensional turbulent boundary-layer development on wings. All three used an eddy viscosity formulation and results from potential flow analysis as external conditions. None of these authors applied his (or her) method to lift loss. The present method achieves considerable simplification with little loss in accuracy by using the three-dimensional integral equations of the boundary-layer flow. Details of the boundary-layer velocity profile that appear in some two- and three-dimensional viscous calculations, e.g., Cebeci et al.,[6] are useful, particularly as regards transition, but are admittedly lost here. However, the gain in ease of use with integral equations is considered to more than compensate inasmuch as the integral properties of the boundary layer, particularly δ^*, suffice for the prediction of lift loss. Cumsty and Head[7] used the integral form of the boundary-layer equations as derived by Cooke and Hall[8] to predict the boundary layer on an infinite swept wing. The present method parallels this work but is not restricted to infinite span, so that the boundary-

Received Dec. 19, 1996; revision received July 8, 1997; accepted for publication July 9, 1997.

*Aerodynamicist, Aerodynamics Laboratory, Institute for Aerospace Research.

layer flow is described by partial, not ordinary, differential equations, and this feature admittedly requires some care in their solution.

Model

A streamline coordinate system (s, n) in the wing surface is used to calculate the development of the boundary layer, s being the distance along a streamline, n being the distance along an orthogonal, and z being the distance normal to the surface. The three-dimensional momentum integral equations of the turbulent boundary-layer flow as presented in Cumsty and Head[7] are as follows:

$$\frac{\partial \Theta_{11}}{\partial s} + \frac{\partial \Theta_{12}}{\partial n} + \frac{\Theta_{11}}{U}\frac{\partial U}{\partial s}(2 + H) + (\Theta_{11} - \Theta_{12})\frac{\partial \gamma}{\partial n} = \frac{c_f}{2} \tag{1}$$

$$\frac{\partial \Theta_{21}}{\partial s} + \frac{\partial \Theta_{22}}{\partial n} + \frac{2}{U}\frac{\partial U}{\partial s}\Theta_{21} + \frac{\Theta_{11}}{U}\frac{\partial U}{\partial n}\left(1 + H + \frac{\Theta_{22}}{\Theta_{11}}\right) + 2\frac{\partial \gamma}{\partial n}\Theta_{21} = c_f \tan \beta/2 \tag{2}$$

Cumsty and Head[7] used Head's entrainment equation (Ref. 9) in three-dimensional form as the auxiliary equation. In this paper, it is written as follows:

$$\frac{\partial(\delta - \delta_1^*)}{\partial s} - \frac{\partial \delta_2^*}{\partial n} = F(H_{\delta - \delta_1^*}) - (\delta - \delta_1^*)\left[\frac{\partial U}{U \partial s} + \frac{\partial \gamma}{\partial n}(1 - e)\right] \tag{3}$$

where, following Crabbe,[10] e is 0.5 in diverging flow, $\partial\gamma/\partial n > 0$ and 0.1 in converging flow, and $\partial\gamma/\partial n < 0$, where $\partial\gamma/\partial n$ is the divergence of the potential flow in the plane of the surface. Figure 1 illustrates streamline divergence. s and n form a curvilinear orthogonal coordinate system where it is readily seen that when the difference in the direction of two adjacent streamlines increases by $d\gamma$ in a crossflow distance of dn, the streamline divergence is $\partial\gamma/\partial n$.

The Θ_{ij} and δ_j are the various integral thicknesses, as follows:

$$\Theta_{11} = \int_0^\delta \frac{u}{U}\left(1 - \frac{u}{U}\right) dz, \qquad \Theta_{12} = \int_0^\delta \frac{v}{U}\left(1 - \frac{u}{U}\right) dz$$
$$\Theta_{21} = -\int_0^\delta \frac{uv}{U^2} dz, \qquad \Theta_{22} = -\int_0^\delta \frac{v^2}{U^2} dz \tag{4}$$
$$\delta_1^* = \int_0^\delta \left(1 - \frac{u}{U}\right) dz, \qquad \delta_2^* = -\int_0^\delta \frac{v}{U} dz$$

Cumsty and Head[7] showed that Mager's profile[11] for the crossflow

$$v/u = (1 - z/\delta)^2 \tan \beta \tag{5}$$

and Cumsty and Head's form[7] for the streamwise velocity profile

$$u/U = (z/\delta)^{(H-1)/2} \tag{6}$$

are reasonably close to observation. Equations (4–6) enable the crossflow integral thicknesses to be simply expressed as functions of H, Θ_{11}, and tan β. In these equations, U is the resultant potential surface fluid velocity along a streamline, and H is δ_1^*/Θ_{11}, i.e., the ratio of streamwise displacement thickness to streamwise momentum thickness.

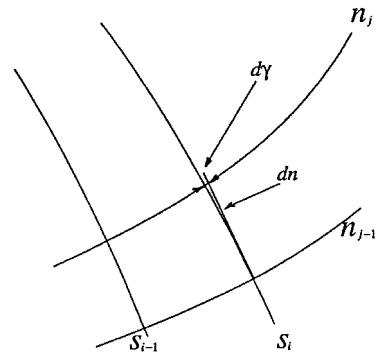

Fig. 1 Streamline divergence.

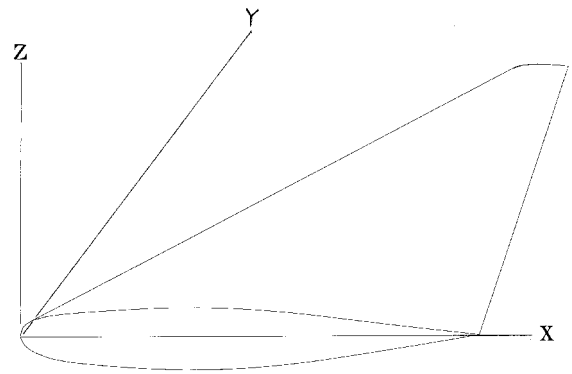

Fig. 2 Global coordinate system.

The equation for the skin friction coefficient is taken from Dvorak[12] to be able to accommodate rough surfaces in terms of roughness height k and dimensionless spacing λ:

$$c_f = c_f(H, \Theta_{11}, k, \lambda) \tag{7}$$

However, in this paper, boundary-layer computations are performed for smooth surfaces only. Fully turbulent flow is assumed. Although it is likely that the boundary layer will be laminar on the lower surface, it is unlikely that the lift loss will be affected by the assumption of turbulent flow here. Calculations[2] for the case of an NACA 0012 airfoil at an angle of attack of 10 deg and a Reynolds number of 2.9×10^6 reveal that the viscous lift loss is 5.0% when transition is forced at 4% chord and the calculations are almost the same, 5.1%, when the transition is forced at 96% chord.

The formula for orthogonal derivatives is derived from simple linear transformation. Thus, if $\nabla = i_x(\partial/\partial x) + i_y(\partial/\partial y)$, where x and y are local Cartesian coordinates in the wing surface (x is parallel to the X–Z plane in Fig. 2 and z is the outward normal to the surface), and if $\gamma = \tan^{-1}(U_y/U_x)$, then

$$\frac{\partial}{\partial n} = -\sin \gamma \frac{\partial}{\partial x} + \cos \gamma \frac{\partial}{\partial y} \tag{8}$$

The external flow (U_x, U_y) in the x and y directions, respectively, is known from the potential flow solution. The potential surface flow was calculated using Panel Method Aerodynamic Laboratory (PMAL) (Ref. 2) using 50 chordwise panels whose chordwise dimensions have a cosine variation and seven spanwise strips whose width is uniform, for a total of 350 panels altogether per half wing (the other half was handled by reflection as was ground effect). Numerical tests indicated that this density of paneling brings the computed potential lift coefficient to within 2.0% of its asymptotic value. Although developed independently, PMAL predicts potential values of

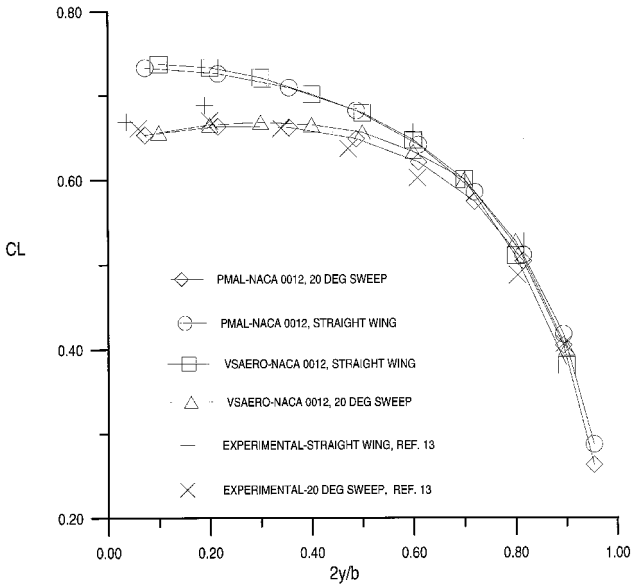

Fig. 3 Span loading on a NACA 0012 wing.

wing lift similar to those from VSAERO (Fig. 3). In Fig. 3, the aspect ratios are 5.9 for the straight wing and 5.6 for the swept wing. The VSAERO and experimental data were taken from Margason et al.[13]

Method of Solution

Numerical Scheme

Most numerical methods for solving nonlinear differential equation sets rely on uniform step size, whereas step size distribution in the present surface panel grid is closer to cosine. Uniform size was achieved, however, by dividing each step along a streamline into four equal parts and applying fourth-order Runge–Kutta to advance the numerical solution to the three-fourths point. The solution was then advanced to the end of the step using the Adams–Bashforth–Moulton predictor–corrector method. The overall scheme is therefore a mix of explicit and implicit operations, but it appears to be efficient and robust.

Equations (1–3) were solved using the preceding scheme along two streamlines, one on each of the upper and lower surfaces of the wing, in each of the seven chordwise strips, starting at the flow attachment line. Two nested computational loops were used. The outer loop is between the potential flow solution and the boundary-layer flow solution, whereas the inner loop for the boundary-layer flow begins in each case by ignoring orthogonal derivatives of the crossflow integrals and then including them in the second and higher passes after the streamwise boundary-layer flow is computed. These orthogonal derivatives are small relative to the streamwise derivatives as shown by a simple order-of-magnitude analysis

$$\frac{\partial}{\partial n}\Big/\frac{\partial}{\partial s} = \mathbb{O}(1/\mathrm{AR})$$

Consequently, multi-inner-loop passes were not observed to substantially change the result. In fact, after only about five outer-loop passes and three inner-loop passes in a straight wing calculation, changes in wing lift coefficient were no larger than about 0.5% per iteration. In each iteration, PMAL changes the surface source strengths incrementally by the amount $d\sigma = \partial(U\delta^*)/\partial s$ (Ref. 14). Damping was provided via a relaxation coefficient, $\omega = 0.5$, so that the new value of σ is given by

$$\sigma^i = \sigma_0 + \omega\, d\sigma + (1 - \omega)\, d\sigma^{i-1} \tag{9}$$

where σ_0 is the potential value of σ, and i is the iteration number. In these expressions, δ^* is defined by

$$\delta^*(s) = \delta_1^* + \frac{\partial}{U\partial n}\int U\delta_2^*\, ds \tag{10}$$

following Lighthill,[14] where δ_2^* is the crossflow (orthogonal) displacement thickness. Iterations continued until successive wing lift coefficients differed by less than 0.3%.

Modification of Trailing-Edge Pressure

Preliminary numerical computations revealed that the turbulent boundary separated in the highly adverse surface pressure gradient predicted by PMAL near the trailing edge of a wing having a finite trailing-edge angle, even at modest angles of attack. This result suggests that the actual trailing-edge pressure coefficient on a wing (*cpte*) is less than unity. Calculations in Crabbe[2] for an airfoil at high angles of attack with surface contamination predicted maximum lift coefficients very close to measured values using a value of *cpte* = 0. At lower angles of attack, data in Ref. 15 reveal slightly positive values of *cpte*, at least for an airfoil. Some care appeared to be warranted, therefore, in modeling the trailing-edge pressure on a wing flying from climb to cruise conditions (C_L from about 1.0 to 0.3) when computing turbulent boundary development.

The three-dimensional code was therefore modified to replace the computed surface pressure distribution near the wing-trailing edge (*xte*) by a function that reproduces the computed surface pressure and pressure gradient near the trailing edge and proceeds smoothly to the value of *cpte* chosen. In keeping with the philosophy of the present method, a single value independent of spanwise location and angle of attack was sought on the grounds that to allow such dependencies appeared to be an unnecessary refinement at this stage. Moreover, surface pressure data on the NACA 0012 wing in Yip and Shubert,[16] and to a lesser extent on the NASA LS(1)-0417 wing in Kjelgaard and Thomas,[1] support the notion of a single value of *cpte* for the wing, independent of spanwise location and angle of attack below stall.

A simple equation for the modified surface pressure distribution near the trailing edge, valid for $cp \le 1$, is as follows:

$$cp(x/c) = cp(x\phi/c) + (x/c - x\phi/c)cp'(x\phi/c) + a(xte - x\phi/c)\ell n\cosh[4(x/c - x\phi/c)/(xte - x\phi/c)] \tag{11}$$

where

$$a = [cpte - cp(x\phi/c) - (xte - x\phi/c)cp'(x\phi/c)]/[(xte - x\phi/c)\ell n\cosh 4]$$

Equation (11) was coded into the boundary-layer component of PMAL with the onset of the modification, at $x/c = x\phi/c$, automatically computed to minimize the difference between original and modified surface pressure distributions near the trailing edge. The modification was observed to alter the potential lift coefficient by only about 0.5%, or about one-tenth of the expected viscous lift loss. The code was then run for several nearly straight wings possessing moderately thick airfoils and varying degrees of taper and twist, and the value of *cpte*, which gave agreement between predicted and measured lift curve, was recorded. The results are plotted in Fig. 4 with the mean value, 0.2447, shown. This value of *cpte* is reasonably close to that measured in Yip and Shubert[16] as well as in Kjelgaard and Thomas.[1] An example of the resultant surface pressure distribution at an angle of attack = 8 deg and $2y/b$ = 0.29 appears in Fig. 5 for the NACA 0012 wing in Yip and Shubert.[16] $X\phi/c$ is about 0.75 and the average value of *cpte*, 0.2447, was used. Because there is very little dispersion of

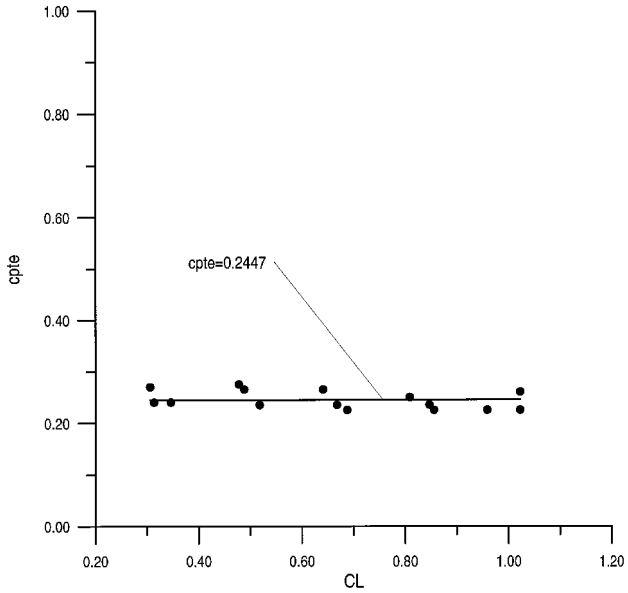

Fig. 4 Value of *cpte* for use in model.

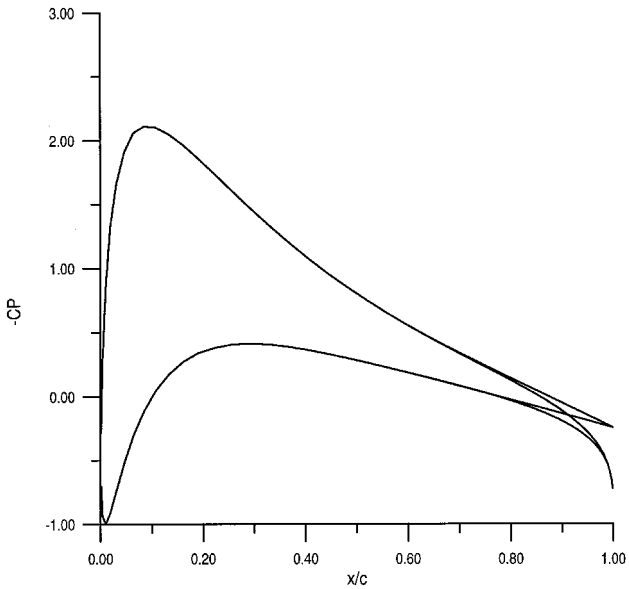

Fig. 5 Modified pressure distribution in viscous flow, α = 8 deg.

computed values about the mean and the mean does not disagree with observation, the mean value so computed, 0.2447, is adopted as the trailing-edge pressure coefficient in the present model together with Eq. (11).

This value of *cpte* may be considered to be the largest value of the trailing-edge pressure coefficient for fully attached flow, at least over the linear part of the lift curve. There may, however, be cases where either a thin wing section and/or substantial leading-edge sweep results in potential values of *cpte* less than 0.2447. The value of *cpte* for use in the model is then the smaller of 0.2447 with Eq. (11) and the value deriving from the unmodified flow solution.

Applications

The method previously described is applied to the computation of the lift curve of five wings, the first two being nearly straight with moderately thick airfoils, having been used to generate the data in Fig. 4. The first is AR 5.9, constant chord, and zero sweep, taper, and twist. The wing section is a NACA 0012, and the chord Reynolds is 4.7×10^6. Experimental data appear in Yip and Shubert.[16]

The second example is the tapered fighter aircraft wing of AR 6, aerodynamic twist of 2.3 deg per meter span, quarter-chord sweep of 3.18 deg, and taper of 0.5 reported in Pearson et al.[17] The mean chord Reynolds number was 3×10^6. The wing section is a NACA 23016 at the root tapering to a NACA 23009 at the tip.

Examples three to five feature swept wings of thinner section. The third example is the highly aft-loaded wing of AR 8.35, taper of 0.35, and quarter-chord sweep of 28 deg, measured in Lovell.[18] A 10.7% NPL airfoil was employed and the mean chord Reynolds number was 1.6×10^6.

The fourth example is the thin, highly swept, tapered wing of AR 4, taper of 0.6, and quarter-chord sweep of 45 deg described in Racisz and Paradiso.[19] A NACA 2-006 airfoil was employed and the mean chord Reynolds number was 6×10^6. This reference also contains wind-tunnel data on lift curve at a lower Reynolds number, but the data are contaminated by the presence of a leading-edge vortex.

The final example is the highly swept constant chord wing of zero taper, AR 5, and sweep of 45 deg measured in Brebner and Wyatt.[20] The chord Reynolds number was 2.1×10^6 and the airfoil section an RAE101 of 12% thickness.

Results

Model results for the first two examples are compared to measurements (in the second example, at the lowest Mach number reported, 0.2) in Figs. 6 and 7. The agreement shown is obtained using the average value of the trailing-edge pressure coefficient appearing in Fig. 4, 0.2447. Thus, a value of *cpte* = 0.2447 in Eq. (11) could be used for preliminary estimates of viscous lift loss of nearly straight wings in incompressible flow during the climb and cruise portions of the flight whenever the computed trailing-edge pressure coefficient is larger than 0.2447.

As indicated earlier, the last three examples are cases where the computed trailing-edge pressure coefficient is smaller than 0.2447 so that the model used the unmodified trailing-edge pressure distribution. The results are plotted in Figs. 8–10. The agreement here is almost as good as in the first two examples, although the model fails to accurately predict the lift coefficient above an angle of attack of about 6 deg in the fifth example. The reason for this discrepancy is not known except that the experimental lift curve in Brebner and Wyatt[20] displayed an unexplained break in slope at about 5 deg angle of attack.

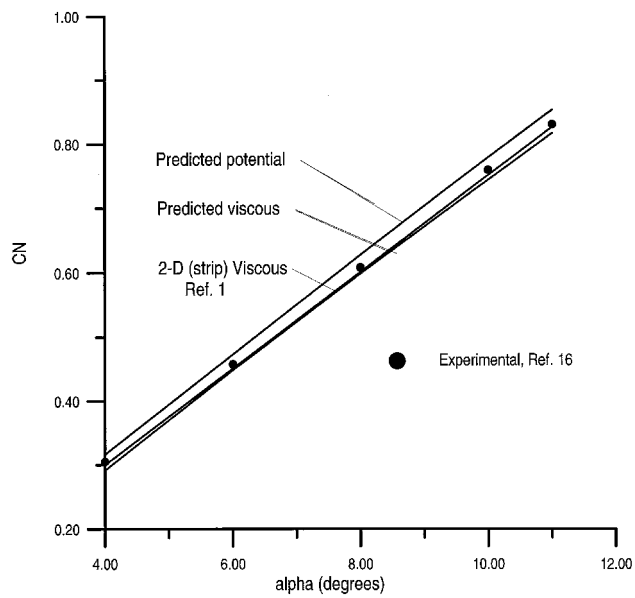

Fig. 6 Lift curve of the NACA 0012 wing, prediction vs observation.

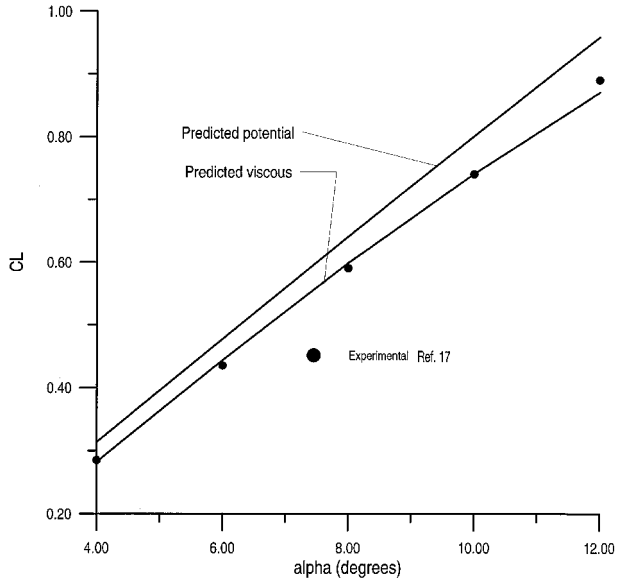

Fig. 7 Lift curve of the NACA 23016 wing, prediction vs observation.

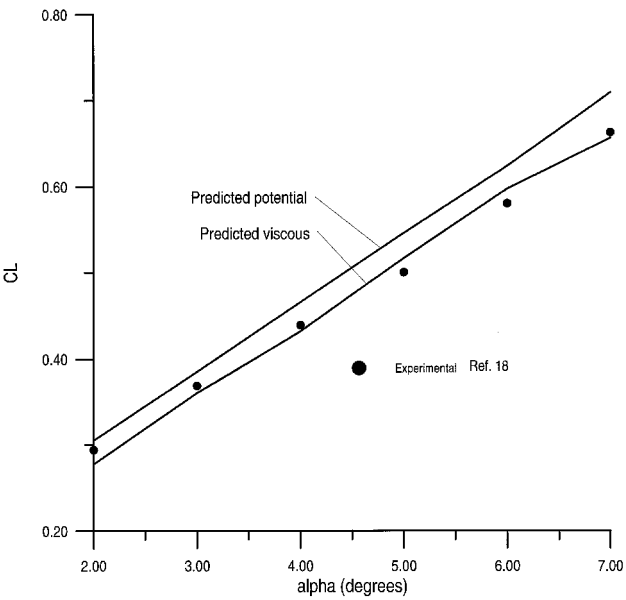

Fig. 8 Lift curve of the NPL wing, prediction vs observation.

Figure 6 also contains the prediction of the two-dimensional strip boundary-layer method of Ref. 1. Both methods predict the viscous lift coefficient satisfactorily, the two-dimensional strip method being somewhat closer to experimental values. The small difference that exists may be a result of the Ref. 1 computation of the lift coefficient, CL, rather than the normal force coefficient, CN, which is used both in Ref. 16 and in the present paper for this particular case. Also, in this particular case, 80 in lieu of 50 panels were used because two different boundary-layer methods were being tested. In a recent paper, Cebeci[21] also uses strip theory for boundary-layer prediction on a wing and reports little difference between that and a quasi-three-dimensional prediction method.

Three-Dimensional Flow Separation

The full three-dimensional method of this paper computes the direction of the wall shear-stress vector, and so it is more appropriate for prediction of the three-dimensional flow separation line following the method in Ref. 7. A plot of the computed wall shear-stress direction with respect to X/c on the upper surface of the F28 MK1000 wing[22] at takeoff at 70

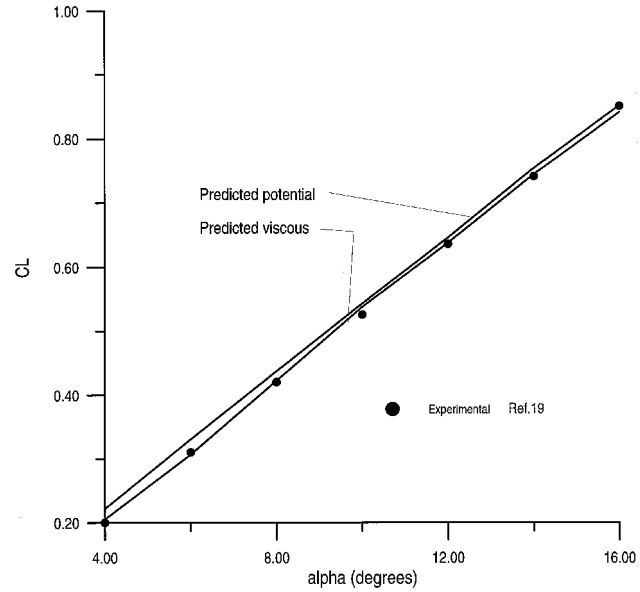

Fig. 9 Lift curve of the NACA 2-006 wing, prediction vs observation.

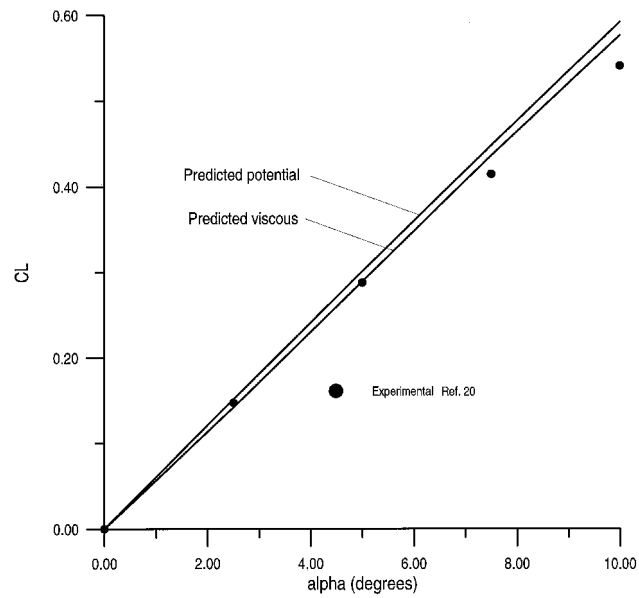

Fig. 10 Lift curve of the RAE101 wing, prediction vs observation.

ms^{-1}, just outboard the 18-deg-deflected flap, is given in Fig. 11. Flow separation, for this case of the wing root angle of attack of 12.5 deg, is predicted using Maskell's criterion[23] to be at 98% chord where the wall shear direction is approaching the direction of a wing generator ($\pi/2 + \lambda te$). The three-dimensional boundary-layer displacement thickness [Eq. (10)] is also plotted, showing rapid growth near separation. A flapped wing was chosen for this example because the crossflow angles on the wings in this paper were all less than 90 deg.

Two-Dimensional vs Three-Dimensional Computations

The question of whether lift loss should be calculated using two-dimensional (strip) boundary-layer methods, as in Ref. 1, or the full three-dimensional method of the present paper can be answered approximately by examining the lift loss of a high aspect ratio wing. Calculations with the present model for an AR = 20 wing, otherwise similar to that of Ref. 16, reveal that at an angle of attack of 10 deg, the overall wing viscous lift loss is 6.49%, but the lift loss at the first spanwise station,

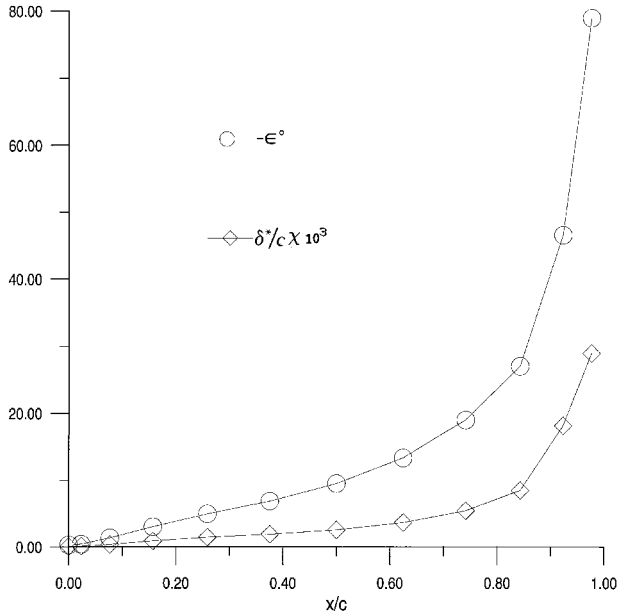

Fig. 11 Three-dimensional boundary layer on F28 wing.

$2y/b = 0.14$, where the boundary layer develops almost two-dimensionally, is 7.32%. This result indicates that two-dimensional computations of wing boundary layers predict a lift loss that is about 10% too high.

Summary and Conclusions

1) A simple numerical model has been presented to compute the loss of lift caused by the incompressible turbulent boundary layer on a wing. The model uses the integral form of the three-dimensional partial differential equations of the boundary-layer flow written in a streamline coordinate system in the wing surface to minimize the crossflow. An in-house low-order surface panel method, PMAL, is used to calculate the wing surface potential flow, and the lift loss is then computed by iteration between the boundary layer and potential flow solutions.

2) When applied to several swept, tapered, twisted wings at incidence, the method predicts the wing lift curve when using either the (average) value of *cpte* = 0.2447 together with the surface pressure modification described [Eq. (11)], whenever the value of *cpte* from the unmodified flow solution is larger, or the unmodified flow solution whenever the value of *cpte* so computed is smaller than 0.2447. The model therefore offers a simple numerical method for initial performance estimates of lift loss during the climb and cruise portions of subsonic flight.

3) Computations with a two-dimensional (strip) model, rather than with the full three-dimensional model of the present paper, will overestimate wing viscous lift loss by about 10%.

4) The integral method yields the local growth in the boundary-layer displacement thickness and the direction of wall shear stress vector, thereby providing a simple method for identifying crossflow separation.

References

[1]Kjelgaard, S. O., and Thomas, J. L., "Comparison of Three-Dimensional Panel Methods with Strip Boundary-Layer Simulations to Experiment," NASA TM 80088, July 1979.

[2]Crabbe, R. S., "Predicted Influence of Fluid Runback Waves on Airfoil Lift," *Proceedings of the 4th Annual Conference of the CFD Society of Canada*, National Research Council, Ottawa, Canada, 1996, pp. 123–126.

[3]Cebeci, T., Kaups, K., and Ramsey, J. A., "A General Method for Calculating Three-Dimensional Compressible Laminar and Turbulent Boundary Layers on Arbitrary Wings," NASA CR-2777, Jan. 1977.

[4]McLean, J. D., "Three-Dimensional Turbulent Boundary Layer Calculations for Swept Wings," AIAA Paper 77-3, Jan. 1977.

[5]Matsuno, K., "A Vector-Oriented Finite Difference Scheme for Calculating Three-Dimensional Compressible Laminar and Turbulent Boundary Layers on Practical Wing Configurations," AIAA Paper 81-1020, June 1981.

[6]Cebeci, T., Chen, H. H., and Arnal, D., "A Three-Dimensional Linear Stability Approach to Transition on Wings at Incidence," AGARD, "Fluid Dynamics of Three-Dimensional Turbulent Shear Flows and Transition," Cesme, Turkey, Oct. 1988.

[7]Cumsty, N. A., and Head, M. R., "The Calculation of Three-Dimensional Turbulent Boundary Layers," *Aeronautical Quarterly*, Pt. 1, Vol. 18, Feb. 1967, pp. 55–84.

[8]Cooke, J. C., and Hall, M. G., "Boundary Layers in Three Dimensions," *Progress in Aeronautical Sciences*, Vol. 2, Pergamon, Oxford, England, UK, 1962.

[9]Head, M. R., "Entrainment in the Turbulent Boundary Layer," Aeronautical Research Council, RC 20, 383, FM 2727, Sept. 1958.

[10]Crabbe, R. S., "A Contribution to the Study of Uniformly Diverging and Converging Turbulent Boundary Layers," Ph.D. Dissertation, McGill Univ., Montreal, PQ, Canada, 1977.

[11]Mager, A., "Generalization of Boundary Layer Momentum Integral Equations to Three Dimensinal Flows Including Those of Rotating Systems," NACA Rept. 1067, 1962.

[12]Dvorak, F. A., "Calculation of Turbulent Boundary Layers on Rough Surfaces in Pressure Gradient," *AIAA Journal*, Vol. 7, No. 9, 1969, pp. 1752–1759.

[13]Margason, R. J., Kjelgaard, S. O., Sellers, W. L., Morris, E. K., Walkey, K. B., and Shields, E. W., "Subsonic Panel Methods—A Comparison of Several Production Codes," AIAA Paper 85-0280, Jan. 1985.

[14]Lighthill, M. J., "On Displacement Thickness," *Journal of Fluid Mechanics*, Vol. 4, 1958, pp. 383–392.

[15]Gregory, N., and O'Reilly, C. L., "Low Speed Aerodynamic Characteristics of NACA 0012 Aerofoil Section, Including the Effects of Upper-Surface Roughness Simulating Hoar Frost," Aeronautical Research Council, R&M 3276, 1973.

[16]Yip, L. P., and Shubert, G. L., "Pressure Distributions on a 1-by 3-Metre Semispan Wing at Sweep Angles from 0 to 40 in Subsonic Flow," NASA TN D-8307, Dec. 1976.

[17]Pearson, E. O., Evans, A. J., and West, F. E., "Effects of Compressibility on the Maximum Lift Characteristics and Spanwise Load Distribution of a 12-Foot-Span Fighter-Type Wing of NACA 230-Series Airfoil Section," NACA A.C.R. L5G10, Nov. 1945.

[18]Lovell, D. A., "A wind-tunnel investigation of the Effects of Flap Span and Deflection Angle, Wing Planform and a Body on the High-Lift Performance of a 28 Swept Wing," Royal Aircraft Establishment, TR 76030, 1976.

[19]Racisz, S. F., and Paradiso, N. J., "Wind-Tunnel Investigation at High and Low Subsonic Mach Numbers of a Thin Sweptback Wing Having an Airfoil Section Designed for Maximum Lift," NACA RM L51L04, Feb. 1952.

[20]Brebner, G. G., and Wyatt, L. A., "Boundary Layer Measurements at Low Speed on Two Wings of 45° and 55° Sweep," Aeronautical Research Council, CP 554, 1961.

[21]Cebeci, T., "An Efficient and Accurate Approach for Analysis and Design of High Lift Configurations," 6th Aerodynamics Symposium, 44th Annual Conf. of the Canadian Aeronautics and Space Inst., Toronto, Canada, April 1997.

[22]Obert, E., "Forty Years of High-Lift R&D—An Aircraft Manufacturer's Experience," CP-515, AGARD, 1993.

[23]Maskell, E. C., "Flow Separation in Three Dimensions," Royal Aircraft Establishment, Rept. Aero 2565, Nov. 1955.